Supporting Information

Multifunctional Colloids with Reversible Phase Transfer between Organic and Aqueous Media *via* Layer-by-Layer Assembly

Miseon Yoon, Jungkyu Choi* and Jinhan Cho*

(a) **(b)**

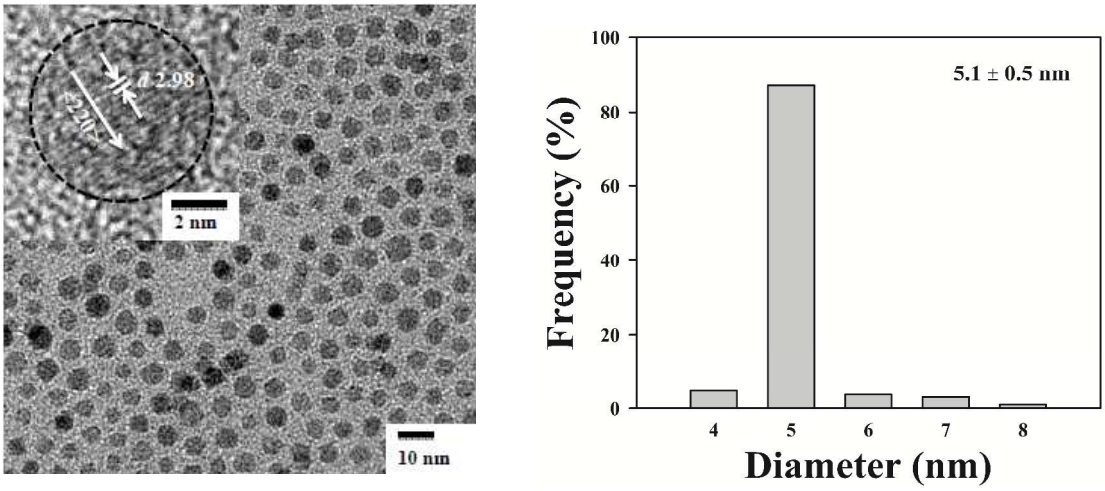

Figure S1. (a) HR-TEM image of OA-Fe_3O_4 with a diameter of approximately 5 nm synthesized in toluene. (b) The size distribution histogram of OA-Fe_3O_4 NPs.

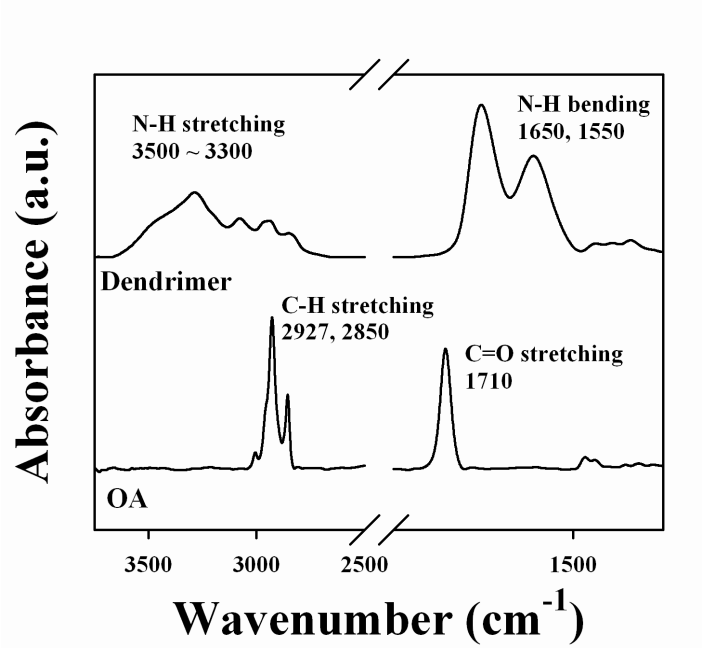

Figure S2. FTIR spectra of dendrimers and pure OA ligands measured from transmission mode

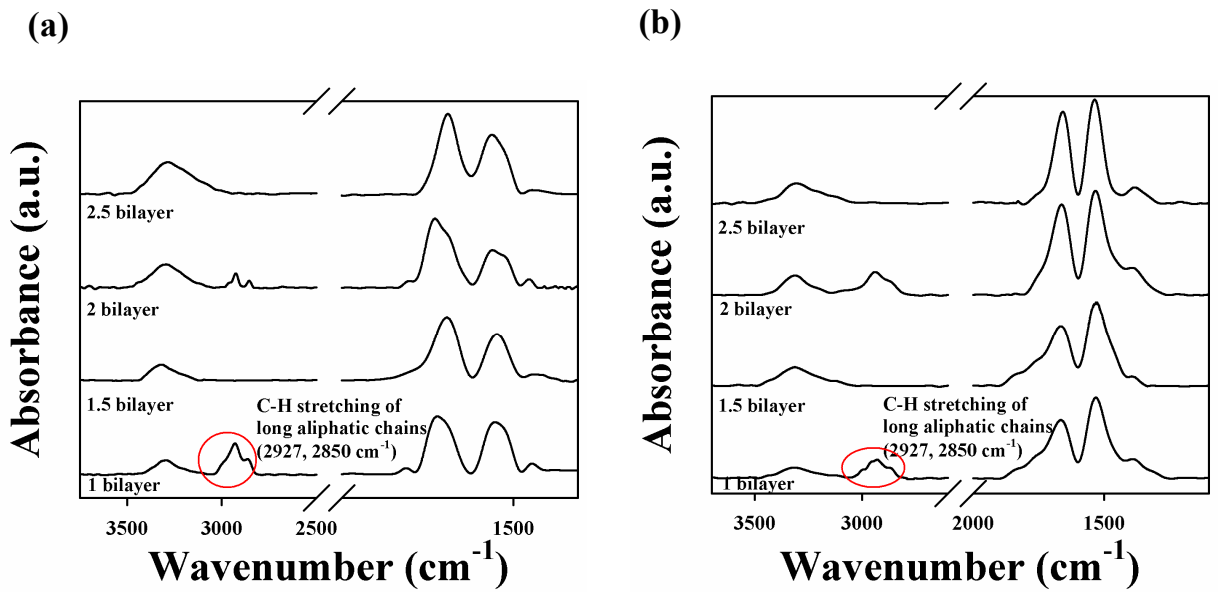

Figure S3. ATR-FTIR-spectra of (a) (dendrimer/OA-Ag_{NP})$_n$ and (b) (dendrimer/TOABr-Au_{NP})$_n$ multilayers as a function of layer number. In the case of (dendrimer/OA-Ag_{NP})$_n$ multilayers, the absorption peaks for C–H stretching (2850 and 2927 cm^{-1}) of the OA ligand containing the long aliphatic chains were observed in ATR-FTIR spectra when OA-Ag_{NP} layer existed as an outermost layer (*i.e.*, 1, 2 and 3 bilayer). On the other hand, in the case of (dendrimer/TOABr-Au_{NP})$_n$ multilayers, the absorption peaks for C–H stretching (2850 and 2927 cm^{-1}) of the TOABr ligand with long aliphatic chains were evidently displayed when the outermost layer was changed from dendrimer to TOABr-Au_{NP} layer (*i.e.*, 1, 2, and 3 bilayered films).

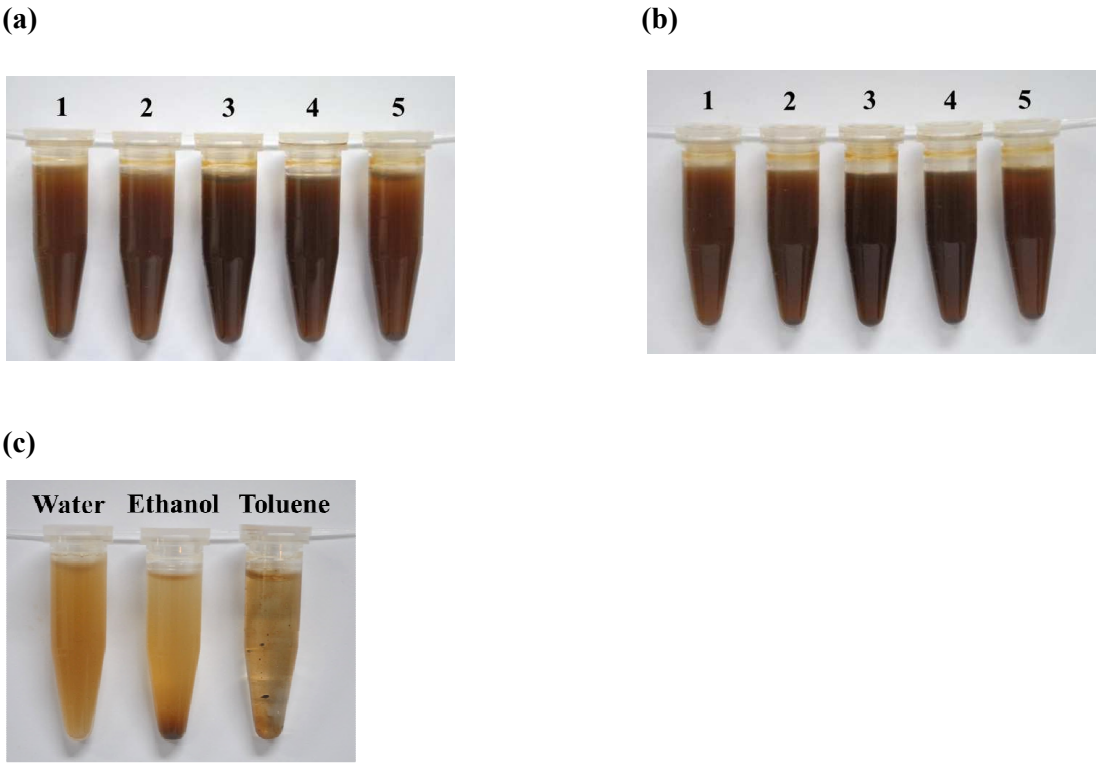

Figure S4. Dispersion stability of (dendrimer/OA–Fe_3O_4 NP)$_9$/dendrimer, or (dendrimer/OA–Fe_3O_4 NP)$_9$ or multilayer-coated silica colloids in various organic media (1: methanol, 2: ethanol, 3. toluene, 4: chloroform, 5: hexane) after (a) 1hr and (b) 1 day. In the case of being dispersed in methanol and ethanol, the top layer of colloids was dendrimer (*i.e.*, (dendrimer/OA–Fe_3O_4 NP)$_9$/dendrimer multilayer-coated silica colloids). On the other hand, the top layer of colloids dispersed in toluene, chloroform, and hexane was OA-Fe_3O_4 NPs (*i.e.*, (dendrimer/OA–Fe_3O_4 NP)$_9$/dendrimer multilayer-coated silica colloids). It should be here noted that the electrostatically charged colloids with poor dispersion stability in organic media were precipitated in a short storage time. As shown in (c), the [(dendrimer/OA–Fe_3O_4 NP)$_9$/dendrimer/(CAT/PAH)$_2$] multilayer-coated colloids with good dispersion stability in aqueous media were rapidly precipitated in ethanol and toluene solvents.

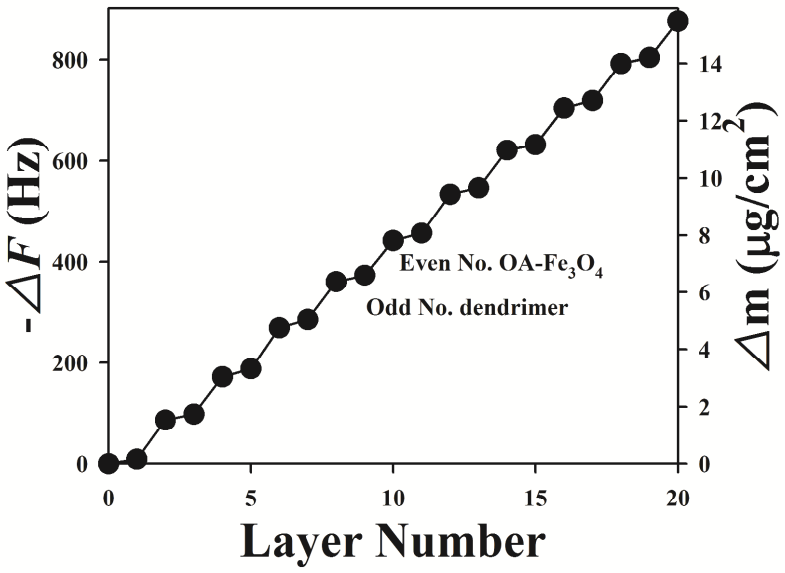

Figure S5. QCM data of (dendrimer/OA-Fe_3O_4 NP)$_n$ multilayers deposited onto flat Au electrode as a function of layer number. Alternating the deposition of the dendrimer and the OA-Fe_3O_4 resulted in $-\Delta F$ of 13 (Δm of ~ 230 ng·cm^{-2}) and 74 Hz (Δm of ~ 1307 ng·cm^{-2}) per layer, respectively

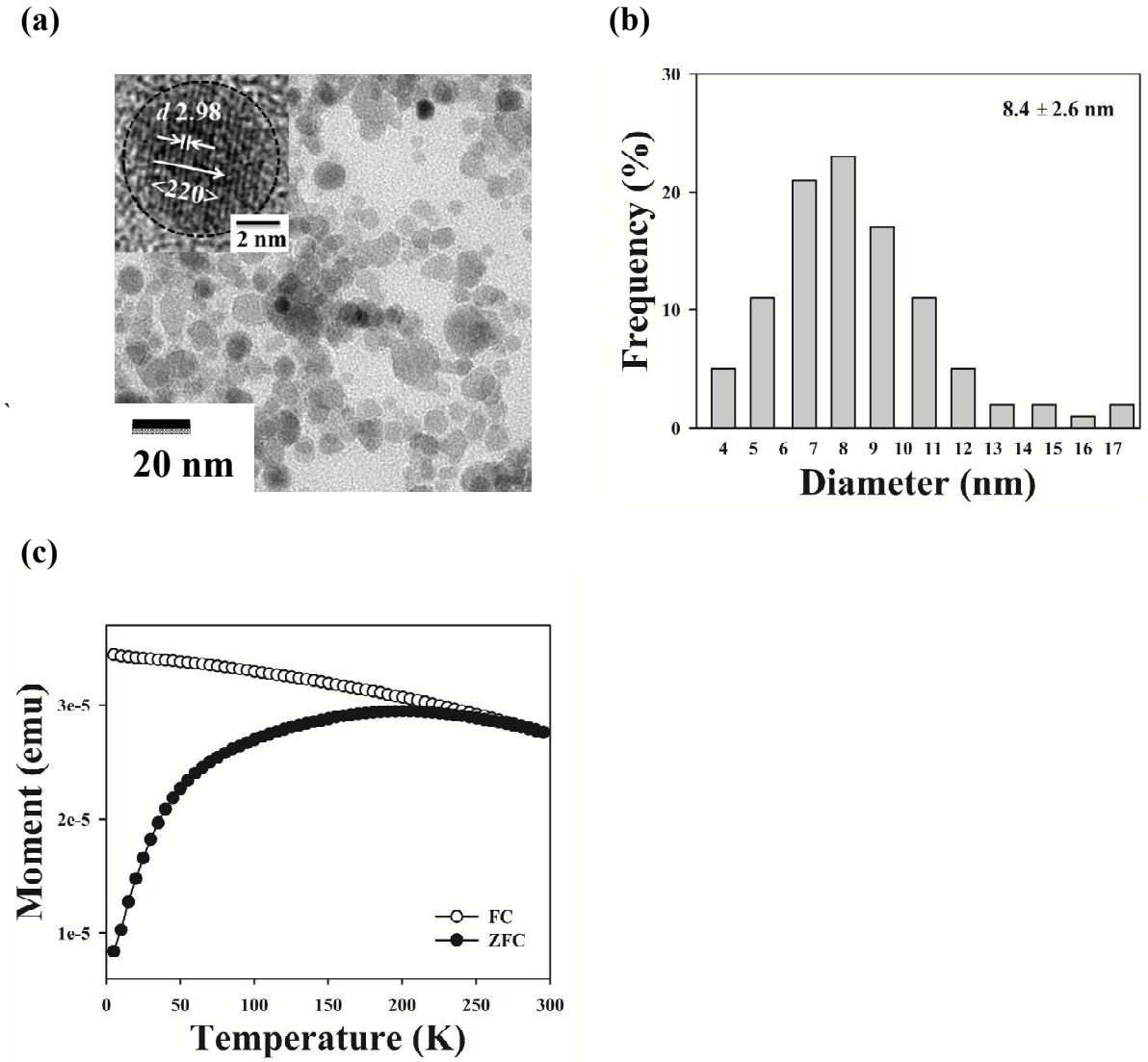

Figure S6. (a) HR-TEM image of anionic Fe_3O_4 NP with a diameter of approximately 8.4 ± 2.6 nm synthesized in aqueous solution. (b) The size distribution histogram of anionic Fe_3O_4 NPs. (c) Temperature dependence of zero-field-cooling (ZFC) and field-cooling (FC) magnetization of anionic Fe_3O_4 NP powder measured at 150 Oe. In this case, we did not observe the evident blocking temperature due to the broad size distribution of anionic Fe_3O_4 NPs.

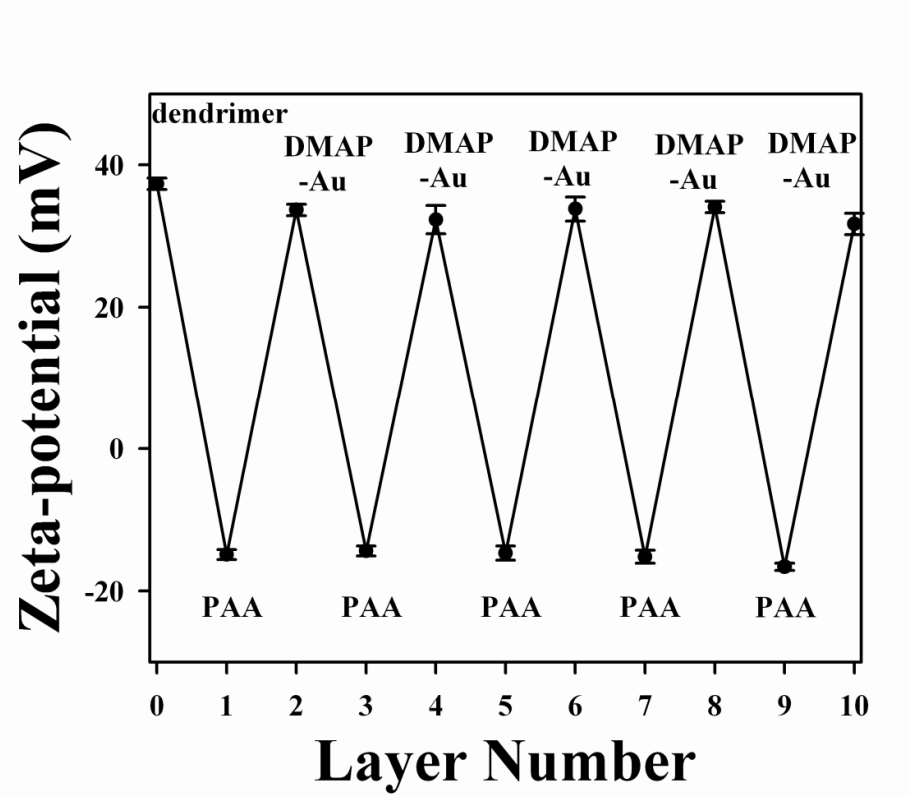

Figure S7. The periodic change in zeta-potential values occurring with the alternating deposition of anionic PAA (at pH 4) and cationic DMAP-Au_{NP} (at pH 4) onto the (dendrimer/OA-Fe_3O_4 NP)$_{4.5}$ multilayer-coated SiO_2 colloids with an outermost dendrimer layer.

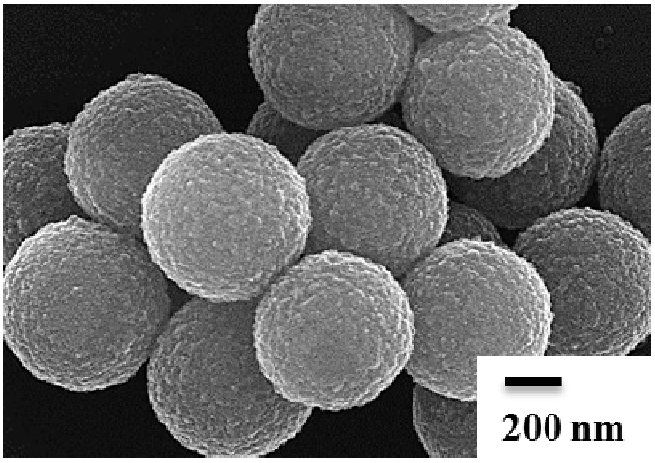

Figure S8. SEM image of (dendrimer/OA–Ag_{NP})$_9$ multilayer-coated colloids

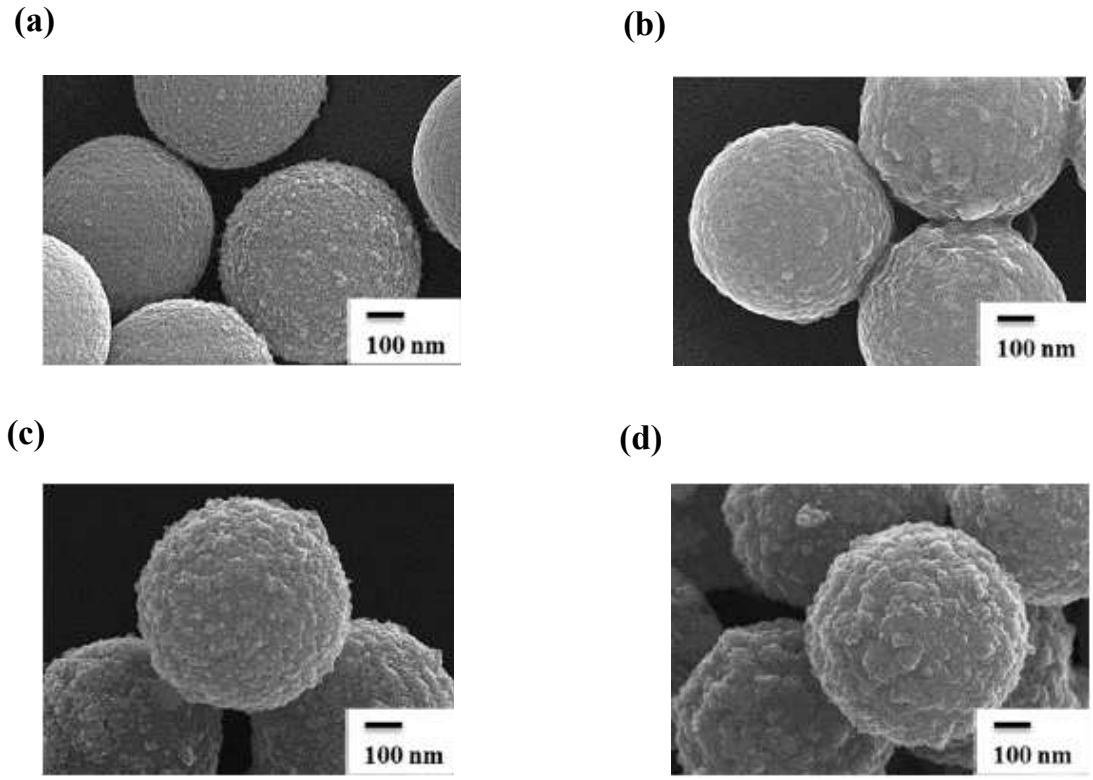

Figure S9. SEM images of (dendrimer/TOA-Au_{NP})$_n$ multilayer-coated colloids; n = (a) 1, (b) 3, (c) 5, and (d) 7.